Acta Crystallographica Section B
Structural Science
ISSN 0108-7681

On the crystal structure of Cr_2N precipitates in high-nitrogen austenitic stainless steel

Tae-Ho Lee,[a]* Chang-Seok Oh,[a] Heung Nam Han,[b] Chang Gil Lee,[a] Sung-Joon Kim[a] and Setsuo Takaki[c]

[a]Materials Processing Department, Korea Institute of Machinery and Materials, 66 Sangnam, Changwon 641-010, Korea, [b]School of Materials Science and Engineering, Seoul National University San 56-1 Sillim, Gwanak, Seoul 151-742, Korea, and [c]Department of Materials Science and Engineering, Kyushu University, 6-10-1 Hakozaki, Higashi-ku, Fukuoka 812-8581, Japan

Correspondence e-mail: lth@kmail.kimm.re.kr

Received 2 September 2004
Accepted 21 December 2004

The crystal structure of Cr_2N precipitates in high-nitrogen austenitic stainless steel was investigated by transmission electron microscopy (TEM). Based on the analyses of selected area diffraction (SAD) patterns, the crystal structure of Cr_2N was confirmed to be trigonal ($P\bar{3}1m$) and was characterized by three sets of superlattice reflections: (001), $(\frac{1}{3}\frac{1}{3}0)$ and $(\frac{1}{3}\frac{1}{3}1)$. These could be explained in terms of the ε-type occupational ordering of nitrogen. The static concentration waves (SCWs) method was applied to describe the ordered superstructure of Cr_2N. The occupation probability function (OPF) for describing the distribution of N atoms in the Cr_2N superstructure was derived based on the superlattice reflections obtained in the SAD patterns and could be expressed as: $n(\mathbf{r}) = c - \frac{1}{6}\eta_1 \cos 2\pi z + \frac{4}{3}\eta_3 \cos(2\pi/3)(x + y + 3z)$. The crystallographic models for ε-type ordering, mainly suggested in the Fe–N system, were discussed in comparison to the present model.

1. Introduction

The crystal structure of Cr_2N has been reported, in most studies (Andrews *et al.*, 1971; Kikuchi *et al.*, 1991; Presser & Silcock, 1983; Simmons, 1995; The Bristol Group, 1984; Vanderschaeve *et al.*, 1995), as hexagonal close-packed (h.c.p.) with the lattice parameters a = 2.748 and c = 4.438 Å. Andrews *et al.* (1971) suggested that the carbides (Mo_2C, Nb_2C and Fe_2C) as well as the nitrides (Cr_2N, Fe_2N and Mn_2N) have the h.c.p. type of structure based on the stacking mode of metal atoms and are designated as the ε-phase. The Bristol group (1984) studied the crystal structure of various precipitates using convergent beam electron diffraction (CBED), and Cr_2N was determined to have the h.c.p. type of structure belonging to the space-group type $P6_3/mmc$. On the contrary, Vallas & Calvert (1985) reported that Cr_2N has a trigonal structure of Pearson's symbol *hp*9 with a = 4.796 and c = 4.470 Å, and belongs to the space-group type $P\bar{3}1m$. Later, Kim *et al.* (1990) confirmed the crystal structure of Cr_2N as trigonal, and refined atomic coordinates together with the occupation parameters using X-ray powder diffraction. Recently, Sundararaman *et al.* (1996) reported that two types of Cr_2N (type A Cr_2N h.c.p. and type B Cr_2N trigonal) were found and the nitrogen ordering caused continuous transformation from type A to type B with aging due to lower misfit strains of type B.

The ε-type occupational ordering of interstitials has been mainly studied in the Fe—N system. Hendricks & Kosting (1930) first suggested that the superlattice reflection $(\frac{1}{3}\frac{1}{3}1)$ found in X-ray powder diffraction could be explained by taking a $3^{1/2} \times 3^{1/2} \times 1$ superstructure based on the geometrical arrangements of Fe octahedra. Later, Jack (1952) confirmed the ε-type ordering for a wide range of Fe—N compositions and proposed a model for a continuous structural transition from ε-Fe_3N to ε-Fe_2N. For compositions close to ε-Fe_3N, a weak superlattice reflection $(\frac{1}{3}\frac{1}{3}0)$ apart from $(\frac{1}{3}\frac{1}{3}1)$ (Hendricks & Kosting, 1930) was observed, and it disappeared gradually with increasing nitrogen contents. Recently, more systematic studies on the ε-type ordering were carried out by Leineweber & Jacobs (2000) and Leineweber *et al.* (2001). They suggested a theoretical model for the interstitial atom arrangement in the ε-type superstructure based on the static concentration waves (SCWs) method (Landau & Lifshitz, 1980; Khachaturyan, 1978, 1983), and investigated the ordering and magnetic properties of ε-type iron-(carbo)nitrides. Although their theoretical model gave useful information on the characteristics of ε-type ordering, the procedure for calculating the interstitial atom occupancy requires some comments related to:

(i) the negative value of the long-range order (LRO) parameter,

(ii) the arbitrary choice of φ and ψ for expressing the symmetry coefficient γ and

(iii) the interstitial redistribution model based on n/η values (the definitions for these parameters are given in Leineweber & Jacobs, 2000).

The objectives of the present study, therefore, are

(1) to clarify the crystal structure of Cr_2N based on the analyses of selected area diffraction patterns (SADPs) with various zone axes,

(2) to elucidate the Cr_2N superstructure in terms of the ε-type occupational ordering and

(3) to derive the modified OPF for describing the distribution of nitrogen in the Cr_2N superstructure using the SCWs method suggested by Landau & Lifshitz (1980), and Khachaturyan (1978, 1983).

2. Experimental

The investigated material was a commercial high-nitrogen austenitic P900NMo alloy (manufactured by VSG, Germany) with the following composition in wt %: 17.94 Cr; 18.60 Mn; 2.09 Mo; 0.89 N; 0.04 C; balance Fe. Specimens were sealed in a quartz tube under vacuum and solution-treated at 1423 K for 30 min in the γ single-phase region (Lee *et al.*, 2004*a*) followed by water quenching. They were then isothermally aged at 1173 K for various times between 10 s and 168 h in an argon atmosphere and quenched into water. Thin foils for TEM were prepared in a twin-jet electrolytic polishing apparatus using a solution containing 15% perchloric acid and 85% methanol. The foils were examined in the JEM 2010 transmission electron microscope at 200 kV. The detailed analyses of SADPs were carried out using Desktop Microscopist V2.2 software (Lucuna Laboratory, USA).

3. Results

3.1. Brief description on the precipitation behavior of Cr_2N

During the isothermal aging at 1173 K, M_2(C, N) (hereafter, simply designated as Cr_2N) precipitation occurred sequentially at the grain boundaries in cellular and, finally, in intragranular form within a matrix. Fig. 1 shows a series of the

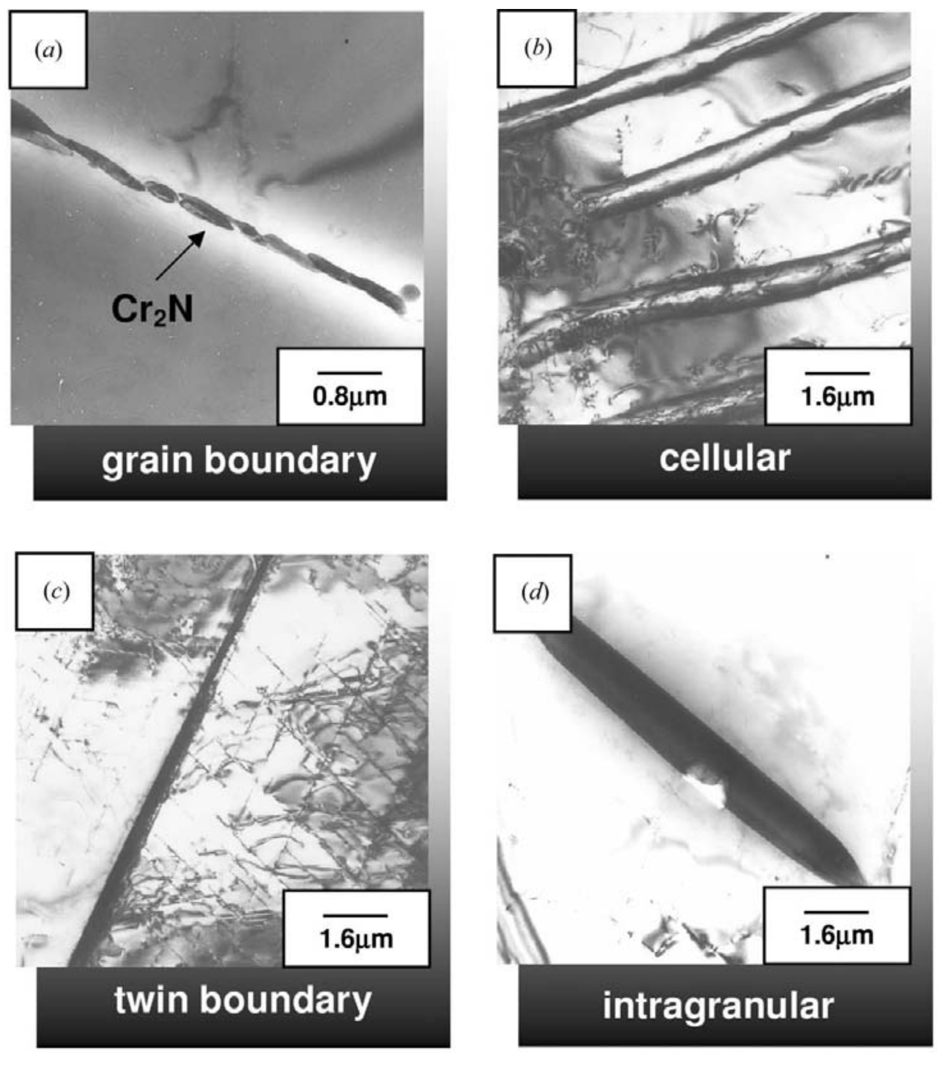

Figure 1
TEM micrographs showing various morphologies of Cr_2N formed during isothermal aging at 1173 K; (*a*) intergranular, (*b*) cellular, (*c*) twin-boundary and (*d*) intragranular Cr_2N, respectively.

bright field (BF) images showing the various morphologies of Cr_2N taken from the specimens aged at 1173 K with various aging times. At an early stage of aging, small needle-like crystals of Cr_2N, with a length of 0.1–0.8 µm, formed along the grain boundaries (Fig. 1*a*), and all the boundaries were covered with precipitates after 10^5 s. After an incubation time of 10^4 s, the cellular precipitation of Cr_2N was initiated from the grain boundaries (Fig. 1*b*) and the volume fraction of cellular Cr_2N increased with age. Long-term aging at 1173 K up to 168 h produced Cr_2N with two distinct morphologies within the grains. Long rod-like Cr_2N with a length of 20–30 µm precipitated along the twin boundary (Fig. 1*c*) and extended over almost the entire grains. In Fig. 1(*d*) the intragranular Cr_2N precipitates formed as platelets with the dimensions 5–10 µm in diameter and 0.1–0.5 µm in thickness. These intragranular Cr_2N precipitates are aligned along the close-packed directions. The detailed descriptions on the precipitation behaviour of the second phases have been given elsewhere (Lee *et al.*, 2004*a*,*b*).

3.2. Crystal structure of Cr_2N

3.2.1. The ε-type occupational ordering of nitrogen. The crystal structures of transition metal carbides/nitrides have been reported on the basis of an h.c.p. metal sublattice in which the interstitial atoms occupy some of the six octahedral interstitial sites (ε-type ordering model): the stacking sequence of the (001)-type plane can be described as follows (Epicier *et al.*, 1988; Hiraga & Hirabayashi, 1980; Lönnberg *et al.*, 1986):

$$A_M \alpha_I B_M \beta_I A_M \alpha_I B_M \beta_I \ldots,$$

where α_I and β_I represent the two types of basal layers occupied by interstitial atoms, and A_M and B_M represent the metal-atom layers. Depending on the distributions of the interstitial atoms, five ordered superstructures [$P\bar{3}m1$, $P\bar{3}1m$ (trigonal), *Pnnm*, *Pbcn* and *Pnma* (orthorhombic)] have been proposed for the M_2X compounds (Epicier *et al.*, 1988; Hiraga & Hirabayashi, 1980).

The schematic illustration of the crystal structure system of Cr_2N ($P\bar{3}1m$) based on the ε-type occupational-ordering model is shown in Fig. 2. The unit cell based on the h.c.p. arrangement of Cr atoms consists of six Cr atoms and six interstitial sites for N atoms and vacancies (Fig. 2*a*). In an ideal close-packed arrangement of Cr atoms, the distance vector between two octahedral sites in the planes α_I and β_I is $c_0/2 \simeq 0.816a_0$, whereas that for two octahedral sites in the same plane is a_0 (a_0 and c_0 are the lattice parameters of the h.c.p. sublattice of the Cr atoms). Thus, it can be deduced that the repulsive interaction for the former is much stronger than that for the latter. This is why one N atom occupies the A1 site in the α_I plane and then the other two N atoms occupy the B2 and C2 sites in the β_I plane in Cr_2N (Fig. 2*c*) (Epicier *et al.*, 1988; Hiraga & Hirabayashi, 1980; Leineweber & Jacobs, 2000; Leineweber *et al.*, 2001). This ε-type occupational ordering of nitrogen leads to an increased superstructure (Fig. 2*b*) (Hiraga & Hirabayashi, 1980; Hendricks & Kosting, 1930; Jack, 1952; Leineweber & Jacobs, 2000) and the new crystal coordinate system based on the N atom at the origin corresponds to the trigonal structure with the space group $P\bar{3}1m$ (Fig. 2*d*).

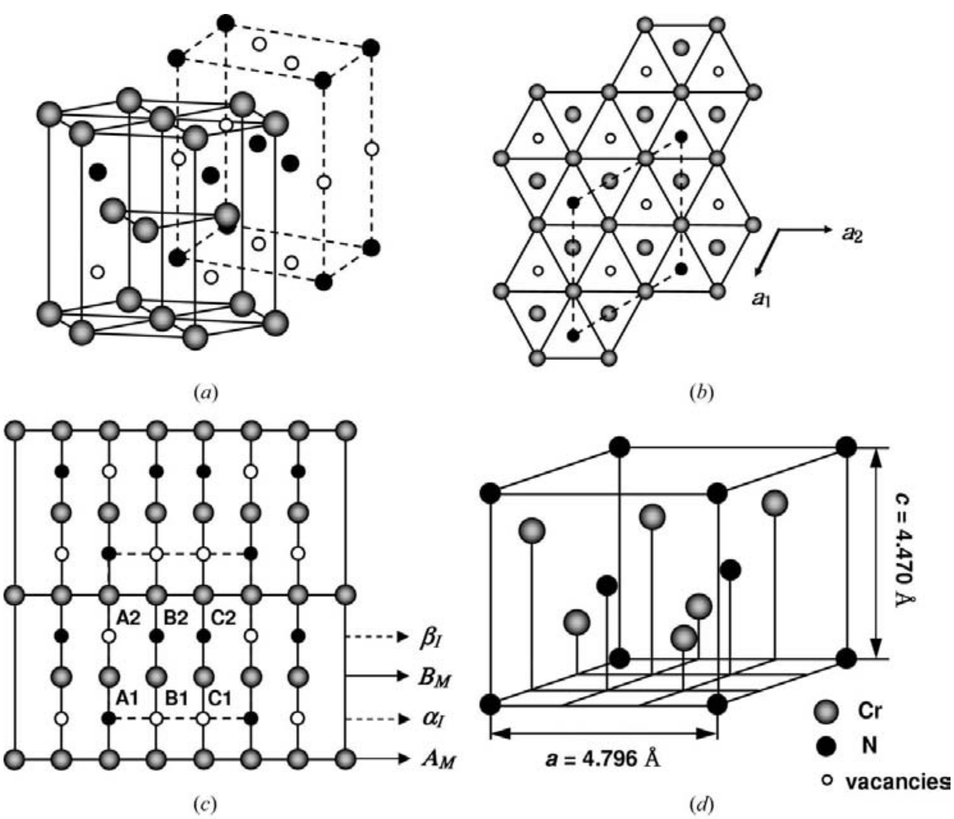

Figure 2
Schematic illustration for the crystal structure of Cr_2N based on ε-type occupational ordering; (*a*) the unit cell based on the h.c.p. arrangement of Cr atoms (for clarity, this is not drawn in a specific crystallographic direction), (*b*) relation of an $(1\bar{1}00)_{\rm hcp}$ to a $3^{1/2} \times 3^{1/2}$ increased unit cell in a [001] projection (the basic hexagonal axes are indicated), (*c*) projection of (*b*) showing six octahedral sites marked A1 to C2, and (*d*) the resultant trigonal unit cell of Cr_2N.

3.2.2. Electron diffraction analysis on the crystal structure of Cr_2N. The crystal structure of Cr_2N has been reported as either h.c.p. or trigonal. In order to clarify which is the correct symmetry, the analyses of SADPs from various zone axes were carried out. Fig. 3 shows the SADPs of Cr_2N with $[1\bar{1}0]$, [001] and [100] zone axes, and the results of a computer simulation based on the data of the h.c.p. structure (open circles; Andrews *et al.*, 1971; The Bristol Group, 1984) and the trigonal structure (filled circles; Kim *et al.*, 1990), respectively. The arrows inserted in SADPs indicate the differences between the h.c.p. and the trigonal structure. Figs. 3(*a*) and (*b*) show the SADP, and the computer-simulated $[100]_{hcp}$ and $[1\bar{1}0]_{tri}$ patterns, respectively. The arrows in Fig. 3(*a*) indicate the reflections of the reciprocal lattice plane of both structures. The scattering intensity of the $(0001)_{tri}$ reflection is calculated to be 2.42 Å, whereas the $(0001)_{hcp}$ reflection is systematically absent. However, it is known that the $(0001)_{hcp}$ reflection can appear in the $[100]_{hcp}$ zone axis due to the double diffraction (Andrews *et al.*, 1971). Thus, the distinction between the h.c.p. and the trigonal structure was not clear in this zone axis.

Figs. 3(*c*) and (*d*) show the [001] SADP of both structures and the results of computer simulation. Besides the h.c.p. reflections with a strong intensity, the $(\frac{1}{3}\frac{1}{3}0)$-type superlattice reflections (for the sake of convenience in the OPF calculation using the SCWs method, the Miller indices for superlattice reflections are written in three digits) were observed along the $\langle 100\rangle_{hcp}$ reciprocal lattice direction and these superlattice reflections correspond to the $\{11\bar{2}0\}_{tri}$ reciprocal lattice plane in the trigonal structure. Figs. 3(*e*) and (*f*) show the SADP, and the results of the calculated $[1\bar{1}0]_{hcp}$ and $[100]_{tri}$ patterns, respectively. All the superlattice reflections distinguishing the h.c.p. from the trigonal structure were identified in this SADP. Apart from the $(\frac{1}{3}\frac{1}{3}0)$ reflection shown in Fig. 3(*c*), two more sets of superlattice reflections, *i.e.* (001) and $(\frac{1}{3}\frac{1}{3}1)$, were observed and these superlattice reflections can be summarized into the three groups shown in Fig. 4.

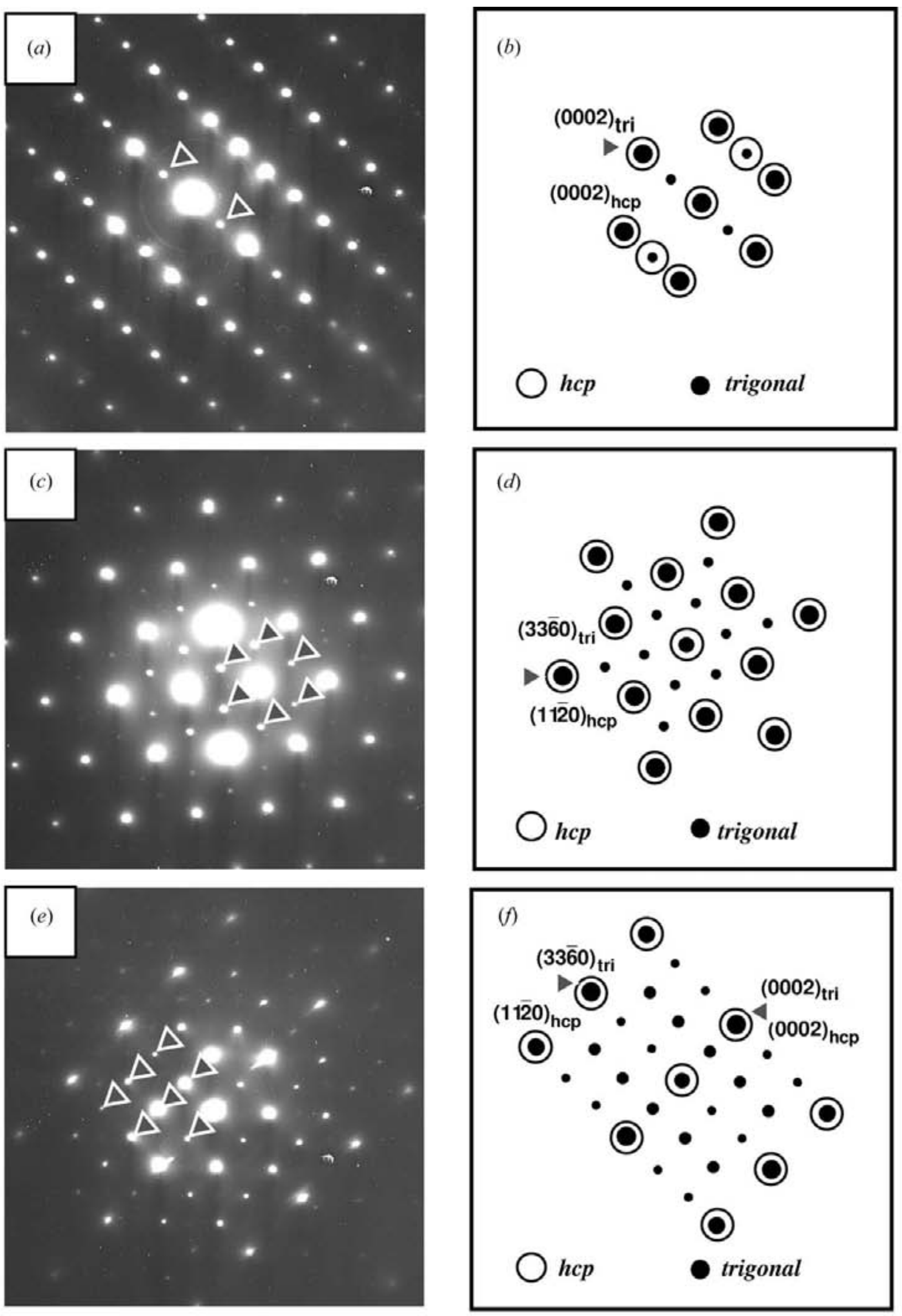

Figure 3
SAD patterns of Cr_2N and the results of computer simulation based on the data of the h.c.p. and trigonal structures; (*a*) SADP ($z = [100]_{hcp}$ and $[1\bar{1}0]_{tri}$), (*b*) results of a computer simulation of (*a*), (*c*) SADP of both structures, (*d*) the results of a computer simulation of (*c*), (*e*) SADP ($z = [1\bar{1}0]_{hcp}$ and $[100]_{tri}$) and (*f*) results of a computer simulation of (*e*), respectively.

Based on the analyses of SADPs and the ε-type ordering model, it can be deduced that:

(i) the h.c.p.-type reflections with a strong intensity correspond to the disordered state of Cr_2N ($P6_3/mmc$), namely, the h.c.p. sublattice of Cr atoms with a random distribution of nitrogen;

(ii) the superlattice reflections that are absent in the h.c.p. structure originate from the occupational ordering of nitrogen in three of six octahedral interstices within the h.c.p. arrangement of Cr atoms, and

(iii) consequently, the trigonal structure ($P\bar{3}1m$), characterized by three sets of superlattice reflections (001), $(\frac{1}{3}\frac{1}{3}0)$ and $(\frac{1}{3}\frac{1}{3}1)$, can be considered to be an ordered version of the disordered h.c.p. structure.

3.3. Description of Cr_2N superstructure using the SCWs method

Based both on superlattice reflections obtained in SADPs and the crystal structure model of Cr_2N in §3.2, the OPF to describe the distribution of N atoms can be derived using the SCWs method. According to Landau & Lifshitz (1980) and Khachaturyan (1978, 1983), if all the positions of the crystal lattice sites $\{\mathbf{r}\}$ are described by one Bravais lattice, the occupation probability for finding an interstitial (substitutional) atom in site $\mathbf{r}$ can be expressed as a superposition of the SCWs

$$n(\mathbf{r}) = c + \tfrac{1}{2}\sum_{s=1}^{s_0} \eta_s[\gamma_s \exp(i\mathbf{k}_0 \cdot \mathbf{r}) + \gamma_s^* \exp(-i\mathbf{k}_0 \cdot \mathbf{r})], \qquad (1)$$

where c is the atomic fraction of the interstitial (substitutional) atoms, $\exp(i\mathbf{k}_0 \cdot \mathbf{r})$ is a SCW, $\mathbf{k}_0$ is a non-zero reciprocal vector of the superlattice reflections located within the first Brillouin zone of the disordered solution, $\mathbf{r}$ is a site vector of the lattice $\{\mathbf{r}\}$, s_0 is the number of superlattice reflections subdividing a fundamental reciprocal lattice vector, η_s is the LRO parameter and γ_s is the coefficient which determines the symmetry of the occupation probabilities with respect to rotation and reflection symmetry operations. In (1) the complex conjugate terms should be contained owing to the symmetry under time reversal, which means that the basis functions of irreducible representation should be real (Landau & Lifshitz, 1980). In the case of the interstitial solution it is assumed that the binary interstitial solution is considered to be the model substitutional one composed of interstitial atoms and their vacancies. The metal-atom configurations need not be taken into account in analyzing an interstitial solution, since they do not take part in the ordering process (Khachaturyan, 1978, 1983).

The schematic illustration of this unit cell is shown in Fig. 5. Moreover, the following two boundary conditions should be satisfied in solving (1) (Khachaturyan, 1978, 1983; Landau & Lifshitz, 1980):

(i) Normalization condition: because of the ambiguous definition of the LRO parameter (η_s), the most frequently used normalization condition is that in a completely ordered state, when $n(\mathbf{r})$ are either zero (vacancies) or unity (occupied by interstitials) on all $\{\mathbf{r}\}$, all the η_s should be equal to unity. This requirement completely defines the values of η_s.

(ii) Conservation of the number of structural degrees of freedom: the total number of $n(\mathbf{r})$ should be greater by unity than the number of LRO parameters.

From the electron diffraction analyses shown in Fig. 3, the superlattice wavevectors corresponding to the (001), $(\frac{1}{3}\frac{1}{3}0)$ and $(\frac{1}{3}\frac{1}{3}1)$ points of the reciprocal lattice are

$$\begin{aligned}\mathbf{k}_1 &= 2\pi\mathbf{a}_3^*,\\ \mathbf{k}_2 &= (2\pi/3)(\mathbf{a}_1^* + \mathbf{a}_2^*) \quad \text{and}\\ \mathbf{k}_3 &= (2\pi/3)(\mathbf{a}_1^* + \mathbf{a}_2^* + 3\mathbf{a}_3^*)\end{aligned} \qquad (2)$$

where $\mathbf{a}_1^*$, $\mathbf{a}_2^*$ and $\mathbf{a}_3^*$ are the reciprocal lattice vectors. Let the lattice site $\mathbf{r}$ be

$$\mathbf{r} = x\mathbf{a}_1 + y\mathbf{a}_2 + z\mathbf{a}_3, \qquad (3)$$

where $\mathbf{a}_1$, $\mathbf{a}_2$ and $\mathbf{a}_3$ are crystal lattice vectors along the (100), (010) and (001) directions, respectively, and x, y and z are coordinates of the interstitial solutions shown in Fig. 5. The scalar product of $\mathbf{k}$ and $\mathbf{r}$ then gives

$$\mathbf{k}_1 \cdot \mathbf{r} = z, \quad \mathbf{k}_2 \cdot \mathbf{r} = \tfrac{1}{3}(x+y) \quad \text{and} \quad \mathbf{k}_3 \cdot \mathbf{r} = \tfrac{1}{3}(x+y) + z. \qquad (4)$$

Substituting (4) into (1) gives the OPF, $n(\mathbf{r})$,

$$\begin{aligned}n(\mathbf{r}) = c &+ \eta_1\gamma_1 \exp(2\pi i z) + \tfrac{1}{2}\eta_2[\gamma_2 \exp\{(2\pi i/3)(x+y)\}\\ &+ \gamma_2^* \exp\{-(2\pi i/3)(x+y)\}]\\ &+ \tfrac{1}{2}\eta_3[\gamma_3 \exp\{(2\pi i/3)(x+y+3z)\}\\ &+ \gamma_3^* \exp\{-(2\pi i/3)(x+y+3z)\}]\end{aligned} \qquad (5)$$

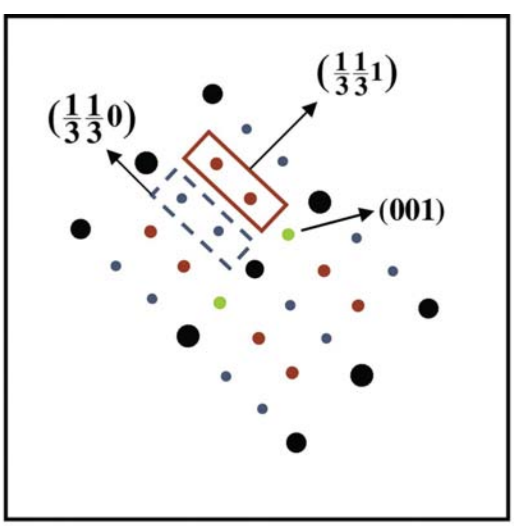

Figure 4
Schematic illustration of the classification of superlattice reflections obtained in the $[100]_{tri}$ zone-axis pattern.

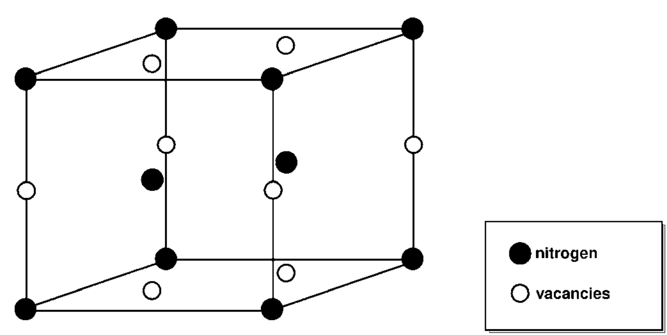

Figure 5
The unit-cell model for the interstitial solution consisting of N atoms and vacancies. The solid and open circles correspond to the N atoms and vacancies, respectively. (This is the same as Fig. 2*d* except that the metal-atom configurations are hidden.)

$$
\begin{aligned}
n(\mathbf{r}) = {}& c + \eta_1\gamma_1\cos(2\pi z) + \\
& \tfrac{1}{2}\eta_2[\gamma_2\{\cos(2\pi i/3)(x+y) + i\sin(2\pi i/3)(x+y)\} \\
& + \gamma_2^*\{\cos(2\pi i/3)(x+y) \\
& - i\sin(2\pi i/3)(x+y)\}] \\
& + \tfrac{1}{2}\eta_3[\gamma_3\{\cos(2\pi i/3)(x+y+3z) \\
& + i\sin(2\pi i/3)(x+y+3z)\} \\
& + \gamma_3^*\{\cos(2\pi i/3)(x+y+3z) \\
& - i\sin(2\pi i/3)(x+y+3z)\}]. \qquad (6)
\end{aligned}
$$

Also, from the lattice coordinate of Cr_2N shown in Fig. 2, six interstitial sites (xyz) can be expressed in terms of the special points in the h.c.p. lattice (Ducastelle, 1991)

$$
\begin{aligned}
& A1: (000), \quad B1: (\tfrac{2}{3}\tfrac{1}{3}0), \quad C1: (\tfrac{1}{3}\tfrac{2}{3}0) \\
& A2: (00\tfrac{1}{2}), \quad B2: (\tfrac{2}{3}\tfrac{1}{3}\tfrac{1}{2}), \quad C2: (\tfrac{1}{3}\tfrac{2}{3}\tfrac{1}{2}). \qquad (7)
\end{aligned}
$$

In a completely ordered state, the normalization condition $c = c_{st}$ (c_{st} is a stoichiometric composition of interstitial solution as shown in Fig. 5), $\eta_s = 1$ and $n(\mathbf{r})$ is either 0 or 1 should be satisfied. Substitution of (7) into (4) gives:

(i) Interstitial sites occupied by nitrogen

$$
\begin{aligned}
n(A1) = {}& \tfrac{1}{2} + \gamma_1 + \tfrac{1}{2}(\gamma_2+\gamma_2^*) + \tfrac{1}{2}(\gamma_3+\gamma_3^*) \\
n(B2) = n(C2) = {}& \tfrac{1}{2} - \gamma_1 + \tfrac{1}{2}\gamma_2[\cos(2\pi/3) \\
& + i\sin(2\pi/3)] + \tfrac{1}{2}\gamma_2^*[\cos(2\pi/3) - i\sin(2\pi/3)] \\
& + \tfrac{1}{2}\gamma_3[\cos(\pi/3) - i\sin(\pi/3)] \\
& + \tfrac{1}{2}\gamma_3^*[\cos(\pi/3) + i\sin(\pi/3)]. \qquad (8)
\end{aligned}
$$

(ii) Interstitial sites corresponding to the vacancies

$$
\begin{aligned}
n(A2) = {}& \tfrac{1}{2} - \gamma_1 + \tfrac{1}{2}(\gamma_2+\gamma_2^*) - \tfrac{1}{2}(\gamma_3+\gamma_3^*) \\
n(B1) = n(C1) = {}& \tfrac{1}{2} + \gamma_1 + \tfrac{1}{2}\gamma_2[\cos(2\pi/3) \\
& + i\sin(2\pi/3)] + \tfrac{1}{2}\gamma_2^*[\cos(2\pi/3) - i\sin(2\pi/3)] \\
& + \tfrac{1}{2}\gamma_3[\cos(2\pi/3) + i\sin(2\pi/3)] \\
& + \tfrac{1}{2}\gamma_3^*[\cos(2\pi/3) - i\sin(2\pi/3)]. \qquad (9)
\end{aligned}
$$

The solution of (8) and (9) is $\gamma_1 = -\frac{1}{6}$, $\gamma_2 = \gamma_2^*$ and $\gamma_3 = \gamma_3^* = 2/3$. In the case of γ_3 and γ_3^* we set $\gamma_3 = \gamma_3^*$ because the final results should be a real number.

Therefore, the generalized OPF for finding an N atom in the site $r = (x\ y\ z)$ can be represented in the form

$$n(xyz) = c - \tfrac{1}{6}\eta_1\cos(2\pi z) + \tfrac{4}{3}\eta_3\cos[(2\pi/3)(x+y+3z)]. \qquad (10)$$

Substituting (7) into (10) gives the OPF, $n(\mathbf{r})$, of Cr_2N four components

$$
\begin{aligned}
& n_1 = c - \tfrac{1}{6}\eta_1 + \tfrac{4}{3}\eta_3, \quad n_2 = c + \tfrac{1}{6}\eta_1 - \tfrac{4}{3}\eta_3, \\
& n_3 = c - \tfrac{1}{6}\eta_1 - \tfrac{2}{3}\eta_3, \quad n_4 = c + \tfrac{1}{6}\eta_1 + \tfrac{2}{3}\eta_3. \qquad (11)
\end{aligned}
$$

This number of components of $n(\mathbf{r})$ satisfies the criterion for the conservation of the number of structural degrees of freedom.

4. Discussion

4.1. Classification of superlattice reflections

In this study three sets of superlattice reflections (001), $(\frac{1}{3}\frac{1}{3}0)$ and $(\frac{1}{3}\frac{1}{3}1)$ were identified in SADPs, which shows that the crystal structure of Cr_2N is trigonal (ordered) rather than h.c.p. (disordered). In this section the classification and definition of these superlattice reflections will be discussed.

(i) Class (001)-type superlattice reflection: This superlattice reflection is known to characterize the ε-M_2X-type superstructures and represents the modulation of the interstitial contents between layers 1 and 2 [n(A1) + n(B1) + n(C1) $\neq$ n(A2) + n(B2) + n(C2); Epicier *et al.*, 1988; Hiraga & Hirabayashi, 1980; Leineweber & Jacobs, 2000]. In the case of Cr_2N shown in Fig. 2(c), this reflection should appear because the N atoms occupy the three interstitial sites A1, B2 and C2. Although the reflection was reported to be characteristic of ε-M_2X, most of the previous studies (Epicier *et al.*, 1988; Hiraga & Hirabayashi, 1980; Hendricks & Kosting, 1930; Jack, 1952) have failed to observe this reflection. On account of the lack of the (001) reflection, some researchers (Epicier *et al.*, 1988; Leineweber & Jacobs, 2000) proposed structures in which the ordering was incomplete with respect to a partial transfer of the C atoms from the $2d$ to the $2c$ site, equilibrating the interstitial contents between layers 1 and 2. Epicier *et al.* (1988) reported that the C atom occupancies in ε-W_2C were determined to be n(A1) = 0.97, n(A2) = 0.03, n(B1 = C1) = 0.26, n(B2 = C2) = 0.74, *i.e.* the carbon contents in layers 1 and 2 were calculated to be 1.49 and 1.51, respectively, and the (001) reflection could not be observed because the difference between the carbon content in these two layers was negligible. On the contrary, this reflection was clearly detected in this study, as shown in Fig. 3. Therefore, in our case, the crystal structure of Cr_2N is perfectly ordered and the occupation probability of the N atoms in B2 and C2 sites is almost 1.

(ii) Class $(\frac{1}{3}\frac{1}{3}0)$-type superlattice reflection: This superlattice reflection is known to characterize the ε-M_3X-type superstructure and reflects the modulation of the interstitial contents between the different channels A, B and C [n(A1) + n(A2), n(B1) + n(B2) and n(C1) + n(C2) become unequal; Leineweber & Jacobs, 2000]. In the case of Cr_2N this reflection did not appear because of the equal nitrogen content between the A, B and C channels, as shown in Fig. 2(c). On the other hand, it is known that this reflection can also appear following the displacement of metal atoms from their ideal positions ($x = \frac{1}{3}$, $y = 0$ and $z = \frac{1}{4}$; Hiraga & Hirabayashi, 1980; Leineweber & Jacobs, 2000) and is especially sensitive to the deviation of the x coordinate. Previous studies have reported that the distortion of the metal atoms from an ideal h.c.p. sublattice was not significant enough to be detected (Leineweber *et al.*, 2001) and the occurrence of this $(\frac{1}{3}\frac{1}{3}0)$ superlattice reflection was restricted only to the characteristics of the ε-M_3X-type superstructure (Epicier *et al.*, 1988; Hendricks & Kosting, 1930; Jack, 1952; Leineweber & Jacobs, 2000). However, it is worthwhile to note that all the ε-type powder samples used in the previous studies (Epicier *et al.*, 1988; Hendricks & Kosting, 1930; Jack, 1952; Leineweber *et al.*, 2001) were obtained in high purity phases with ideal binary metal–interstitial composition; no other alloying elements were involved. On the contrary, the Cr_2N precipitates in the present study are actually M_2X-type compounds composed of several other alloying elements such as Fe, Mo and Mn as substitutional constituents, and carbon as interstitial. On account of this, the partial substitution of Cr atoms by other elements, apart from affecting the interatomic interaction of Cr—N, most likely leads to an additional contribution to the deviation from the ideal h.c.p. arrangement of Cr atoms owing to the displacive scattering process among them. The $(\frac{1}{3}\frac{1}{3}0)$ superlattice reflection found in this study most likely results from the deviation of metal atoms from their ideal positions because of the replacement of some Cr atoms by other substitutional alloying elements and/or the Cr—N atomic interaction. The detailed description on the effect of metal atom displacement caused by a redistribution of N atoms is beyond the scope of this study.

(iii) Class $(\frac{1}{3}\frac{1}{3}1)$-type superlattice reflection: This reflection is known to characterize all the ε-type ordered structures, irrespective of their interstitial contents (Leineweber & Jacobs, 2000; Leineweber *et al.*, 2001). In previous studies (Epicier *et al.*, 1988; Hendricks & Kosting, 1930; Jack, 1952; Leineweber *et al.*, 2001) this reflection was reported to be the only superlattice reflection for the ε-Fe_2N-type superstructure [W_2C, Mo_2C (Epicier *et al.*, 1988), Fe_2N (Hendricks & Kosting, 1930; Jack, 1952)] because of the lack of (001) superlattice reflections. Since the $(\frac{1}{3}\frac{1}{3}1)$ superlattice reflection was common to all types of ε-type ordering, the identification of the ε-Fe_2N-type superstructure, however, could not be achieved. Moreover, the superlattice reflection could have occurred even in the ε-Fe_2N superstructure, resulting from the distortion from an ideal h.c.p. arrangement of metal atoms, especially when the other substutional alloying elements are present in the M_2X compounds, as is the case in this study.

4.2. Crystallographic model for the Cr_2N superstructure

Based on the three sets of superlattice reflections discussed in the previous section, the OPF for the distribution of N atoms in the Cr_2N superstructure can be derived using the SCW's method. In this section the crystallographic model for describing the Cr_2N superstructure will be discussed in comparison with other models (Hendricks & Kosting, 1930; Jack, 1952; Leineweber & Jacobs, 2000; Leineweber *et al.*, 2001).

4.2.1. Earlier models suggested by Hendricks & Kosting (1930) and Jack (1952). Hendricks and Kosting (1930) found the $(\frac{1}{3}\frac{1}{3}1)$ superlattice reflection in the Fe—N system and determined the space groups of Fe_3N and Fe_2N as $P6_322$ (D_6^6) and $P\bar{3}1m$ (D_{3d}^1), respectively, including the ideal atomic positions of iron and nitrogen. Later, Jack (1952) suggested a structural model for the continuous phase transition: ε-Fe_3N $\rightarrow$ ε-Fe_3N_{1+x} $(0 < x < 0.5)$ $\rightarrow$ ε-Fe_2N. Within the unit cell of the ε-type superstructures, one octahedral site is continuously filled with nitrogen in the ε-Fe_3N_{1+x} range and is fully occupied in ideal ε-Fe_2N. However, the space groups of all these nitrides were designated as the lowest symmetry group $P312$ (D_3^1) to describe this continuous structural change. These earlier models require some comments in the light of our recent findings:

(i) All these previous studies failed to observe the existence of the superlattice reflection.

(ii) The super-superstructure $Fe_{24}N_{10}$, proposed by Jack (1952), with the increased unit-cell dimension $2(3^{1/2}) \times 2(3^{1/2}) \times 1$ has not been confirmed in later studies (Epicier *et al.*, 1988; Hiraga & Hirabayashi, 1980; Leineweber & Jacobs, 2000; Leineweber *et al.*, 2001; Lönnberg *et al.*, 1986).

(iii) Although Hendricks and Kosting determined the exact crystallographic data of ε-Fe_3N and ε-Fe_2N superstructures, the superlattice reflection $(\frac{1}{3}\frac{1}{3}0)$ was not detected in ε-Fe_3N powders. Consequently, the only superlattice reflection found in their study was the $(\frac{1}{3}\frac{1}{3}1)$ reflection, which is not enough to distinguish ε-Fe_3N from ε-Fe_2N, as shown in §4.1.

(iv) According to Jack's model, the (000) point of ε-Fe_3N was empty and filled by nitrogen in ε-Fe_2N. However, it is known that these well ordered superstructures can be built on the basis of the h.c.p. sublattice of metal atoms in which some of the octahedral sites are occupied by interstitials. The new crystal coordinate systems based on the N atom at the origin also correspond to ε-Fe_3N ($P6_322$), with an h.c.p. structure, and ε-Fe_2N ($P\bar{3}1m$), with a trigonal structure, respectively (Epicier *et al.*, 1988; Hiraga & Hirabayashi, 1980; Hendricks & Kosting, 1930; Jack, 1952; Leineweber & Jacobs, 2000; Leineweber *et al.*, 2001). Therefore, it is reasonable to build these superstructures taking the N atom at the origin of the atomic coordinate.

4.2.2. Leineweber's model (2000). Leineweber and coworkers (Leineweber & Jacobs, 2000; Leineweber *et al.*, 2001) compiled all the previous ε-type ordering models (Epicier *et al.*, 1988; Hiraga & Hirabayashi, 1980; Hendricks & Kosting, 1930; Jack, 1952) and derived the OPF for describing the interstitial atom distribution in the ε-type superstructures using the SCW method based on Bugaev & Tatarenko's (1989) approach rather than that of Khachaturyan's (1978, 1983) adopted in this study. They suggested the redistribution model of interstitials is a function of calculated n/η values in each octahedral site. However, their approach and the resulting OPF was found to be different from ours in the following ways:

(i) For an ideal ε-Fe_2N superstructure, Leineweber reported that the LRO parameters corresponding to the special positions of the h.c.p. structure (Ducastelle, 1991) were calculated to be $\eta_{K^-} = \frac{2}{3}$, $\eta_{K^-} = 0$ and $\eta_{\Gamma^-} = -\frac{1}{6}$. However, it is known that the LRO parameter should be in the range between 0 (disorder) and 1 (perfect order) (Cullity, 1978). Therefore, the negative value of the LRO parameter is physically unreasonable. This may arise from the assumption that the LRO parameter can be either positive or negative in order to satisfy $\gamma = 1$.

(ii) In the calculation procedure of the n/η values, the angles of φ and ψ were chosen as $\psi = 0$ and π in K^+, and $\varphi = 0$ and $\pi/2$

in K^- special points, respectively. The explanation for this choice, however, was not specified.

(iii) In the interstitial redistribution model for the K^+ point, for example, the authors applied the calculation of n/η_{K+} depending on $\psi = 0$ and π to all six octahedral sites (A1 to C2 sites in Fig. 2*b*). However, the n/η_{K+} value has its meaning only in B1 and C1 octahedral sites, and it is meaningless to apply the calculation of n/η_{K+} to the other four octahedral sites.

In this study the OPF was derived according to Khachaturyan's (1978, 1983) approach and based on the superlattice reflections experimentally obtained in SADPs in order to overcome the problems mentioned in Leineweber's (Leineweber & Jacobs, 2000) model. Khachaturyan (1978, 1983) proposed the formulation of SCWs for describing the distribution of substitutional/interstitial atoms in the ordered cubic system and emphasized the following advantages:

(i) this method formulates the superstructures in terms of the reciprocal lattice providing direct correlation between ordering and diffraction data;

(ii) this method can also provide the symmetry aspects of the order–disorder transition and the structure of the ordered phase can be predicted.

However, in order to apply this method the accurate superlattice reflections should be obtained from experimental methods. Therefore, it can be said that the modified OPF for the Cr_2N superstructure derived in this study is more reliable in that a more general normalization condition was used and the calculation of OPF was based on experimental results.

5. Conclusions

The TEM study on the crystal structure system of Cr_2N precipitates in high-nitrogen austenitic Fe-18Cr-18Mn-2Mo-0.9N steel is summarized as follows:

(i) Based on the careful analyses of SADPs, the crystal structure of Cr_2N was confirmed to be trigonal ($P\bar{3}1m$), including three sets of superlattice reflections (001), ($\frac{1}{3}\frac{1}{3}0$) and ($\frac{1}{3}\frac{1}{3}1$), and could be explained in terms of ε-type occupational ordering of nitrogen.

(ii) The modified OPF for describing the distribution of N atoms in the Cr_2N superstructure was derived using a combination of superlattice reflections in SAD patterns and the SCWs method.

One of the authors (Tae-Ho Lee) wishes to express his sincere thanks to Dr T. Tsuchiyama at Kyushu University, Professor Jongryoul Kim at Hangyang University, Professor Young-Woon Kim at Seoul National University and Mr Hi-Won Jeong at KIMM for helpful discussions, and would like to acknowledge the financial support provided by Japan Society for the Promotion of Science through the dissertation Ph.D program. The authors also would like to express their gratitude to Yeong-Ouk Kim for the TEM observation.

References

Andrews, K. W., Dyson, D. J. & Keown, S. R. (1971). *Interpretation of Electron Diffraction Patterns*, p. 203. London: Hilger.
Bugaev, V. N. & Tatarenko, V. A. (1989). *Interaction and Arrangement of Atoms in Interstitial Solid Solutions Based on Close-Packed Metals.* Kiev: Academy of Sciences.
Cullity, B. D. (1978). *Elements of X-ray Diffraction*, 2nd ed, p. 386. New York: Addison-Wesley Publishing Company, Inc.
Ducastelle, F. (1991). *Order and Phase Stability in Alloys*, p. 162. Amsterdam: Elsevier Science Publishers BV.
Epicier, T., Dubois, J., Esnouf, C., Fantozzi, G. & Convert, P. (1988). *Acta Metall.* **36**, 1903–1921.
Hiraga, K. & Hirabayashi, M. (1980). *J. Appl. Cryst.* **13**, 17–23.
Hendricks, S. B. & Kosting, P. B. (1930). *Z. Kristallogr.* **74**, 511–533.
Jack, K. H. (1952). *Acta Cryst.* **5**, 404–411.
Khachaturyan, A. G. (1978). *J. Prog. Mater. Sci.* **22**, 1–150.
Khachaturyan, A. G. (1983). *Theory of Structural Transformations in Solids*, pp. 39–95. New York: John Wiley.
Kikuchi, M., Kajihara, M. & Choi, S. K. (1991). *Mater. Sci. Eng. A*, **146**, 131–150.
Kim, S. J., Marquart, T. & Franzen, H. F. (1990). *J. Less-Common Met.* **158**, L9–L10.
Landau, L. D. & Lifshitz, E. M. (1980). *Statistical Physics*, Part I, pp. 401–516. Oxford: Pergamon Press.
Lee, T. H., Oh, C. S., Lee, C. G., Kim, S. J. & Setsuo, T. (2004*a*). *Scr. Mater.* **50**, 1325–1328.
Lee, T. H., Oh, C. S., Lee, C. G., Kim, S. J. & Setsuo, T. (2004*b*). *Metals Mater. Inter.* **10**, 231–236.
Leineweber, A. & Jacobs, H. (2000). *J. Alloys Comput.* **308**, 178–188.
Leineweber, A., Jacobs, H., Hüning, F., Lueken, H. & Kockelmann, W. (2001). *J. Alloys Comput.* **316**, 21–38.
Lönnberg, B., Lundström, T. & Tellgren, R. (1986). *J. Less-Common Met.* **120**, 239–245.
Presser, R. & Silcock, J. M. (1983). *Met. Sci.* **17**, 241–247.
Simmons, J. W. (1995). *Metall. Trans. A*, **26**, 2579–2595.
Sundararaman, D., Shankar, P. & Raghunathan, V. S. (1996). *Metall. Mater. Trans. A*, **27**, 1175–1186.
The Bristol Group (1984). *Convergent Beam Electron Diffraction of Alloy Phases*, p. 61. Bristol and Boston: Adam Hilger.
Vallas, P. & Calvert, L. D. (1985). *Pearson's Handbook of Crystallographic Data for Intermediate Phases*, Vol. 2, p. 1877. Ohio: ASM Metals Park.
Vanderschaeve, F., Taillard, R. & Foct, J. (1995). *J. Mater. Sci.* **30,** 6035–6046.